Progress In Electromagnetics Research, Vol. 142, 189–205, 2013

RECONFIGURABLE SIW ANTENNA BASED ON RF-MEMS SWITCHES

Bahram Khalichi*, Saied Nikmehr, and Ali Pourziad

Department of Electrical and Computer Engineering, University of Tabriz, Tabriz, Iran

Abstract—In this article, a novel compact reconfigurable antenna based on substrate integrated waveguide (SIW) technology is introduced. The geometry of the proposed antennas is symmetric with respect to the horizontal center line. The electrical shape of the antenna is composed of double H-plane SIW based horn antennas and radio frequency micro electro mechanical system (RF-MEMS) actuators. The RF-MEMS actuators are integrated in the planar structure of the antenna for reconfiguring the radiation pattern by adding nulls to the pattern. The proper activation/deactivation of the switches alters the modes distributed in the structure and changes the radiation pattern. When different combinations of switches are on or off, the radiation patterns have 2, 4, 6, 8, ... nulls with nearly similar operating frequencies. The attained peak gain of the proposed antenna is higher than 5 dB at any point on the far field radiation pattern except at the null positions. The design procedure and closed form formulation are provided for analytical determination of the antenna parameters. Moreover, the designed antenna with an overall dimensions of only $63.6 \times 50\,\text{mm}^2$ is fabricated and excited through standard SMA connector and compared with the simulated results. The measured results show that the antenna can clearly alters its beams using the switching components. The proposed antenna retains advantages of low cost, low cross-polarized radiation, and easy integration of configuration.

1. INTRODUCTION

Reconfigurable antennas can satisfy three groups of application requirements: resonant frequency [1], polarization [2, 3], and pattern

Received 2 July 2013, Accepted 10 August 2013, Scheduled 25 August 2013

* Corresponding author: Bahram Khalichi (b_khalichi89@ms.tabrizu.ac.ir).

reconfigurability [4–6]. The pattern reconfigurability is one of the most effective methods to improve the performance of a wireless communication system by minimizing interference between users and maximizing signal-to-noise ratio (SNR). In addition, controlling the directions of radiation beams or varying the beam shapes would enhance the performances in radar applications or network control flexibility in wireless communications. Saving energy by aiming signal to the intended users and improving security are other applications of pattern reconfigurable antennas. Consequently, development of reconfigurable pattern antennas with the potential of improving the overall system performances have become an intensive topic in the field of antennas [7–9]. However, conventional reconfigurable pattern antennas require expensive solid-state phase shifters with higher insertion losses as the frequencies increase. Therefore, they are not suitable for low-cost compact commercial applications. Furthermore, microstrip antennas suffer from low efficiency at higher frequencies due to severe power loss caused by conductors and dielectrics. So RF-MEMS actuators with novel SIW technology are good candidates to be replaced with solid phase shifters and microstrips, respectively. They provide advantages of fast actuation and integrated fabrication coupled with attractive options for low-cost high-frequency systems [10–26]. Reconfigurable RF-MEMS antennas were first introduced in 1998 by E. Brown and have been studied by several research groups with emphasizing in reconfigurability of aperture and microstrip antennas [12–14]. Also SIW possesses merits with respect to the conventional rectangular waveguide and has been widely implemented in microwave components and circuit designs [15–26].

In this paper, a novel compact reconfigurable pattern antenna based on SIW technology and usage of integrated RF-MEMS switches is proposed. This antenna has the capacity of reconfiguring the radiation patterns by adding nulls without changing the geometrical parameters and devoid of any impedance matching circuitry. The design analysis is performed by using commercial software, which characterizes 3-D structures in order to determine the bandwidth and radiation pattern of the antenna.

2. SIW HORN ANTENNA DESIGN

One of the simplest and probably the most widely used microwave antennas is the horn [27]. The H-plane SIW based horn antenna has been introduced previously because of its compactness, high gain, planar geometry, and easy fabrication [28, 29]. In addition, horn antennas can be treated as aperture antennas. Therefore, designing

reconfigurable antennas based on SIW technology and RF-MEMS switches are conceivable.

A desired radiation pattern can usually be achieved by an array of radiating elements in an electrical and geometrical arrangement. Specifically, the simplest way to control the characteristics of this radiation pattern is varying the separation and/or phase between the elements [27]. In this paper, a novel antenna constituting two H-plane SIW based horn antennas is proposed. A 3-D configuration of the proposed antenna is shown in Figure 1. In this antenna, the combination of the electric and magnetic current elements at the apertures with different spacing can create different patterns. Therefore, The spacing between apertures determines the number of major lobs and nulls. The whole antenna was designed on a single Rogers 5880 substrate with a relative permittivity of 2.2 and a thickness of 1.6 mm. It has already been demonstrated that, if the leakage loss of the SIW is near to zero, SIW would act similar to a dielectric filled rectangular waveguide [15]. Therefore, in designing procedure, considering the role of SIW as a rectangular waveguide, makes the analysis of the structure easier than full wave analysis. Local coordinate systems (x', y', z') and (x'', y'', z'') are considered at the locations of apertures 1 and 2, respectively. Considering the role of SIW as conventional dielectric-filled rectangular waveguide, the fields at the apertures of the horns can be obtained by treating the horns as radial waveguides [27]. The fields within the horns can be expressed in terms of cylindrical TE wave functions which include Hankel functions (TM waves are not supported by SIW structures). So the fields on the surface of the apertures are combination of the TE_{n0} modes. By simplifying Hankel function, the tangential fields at the first aperture

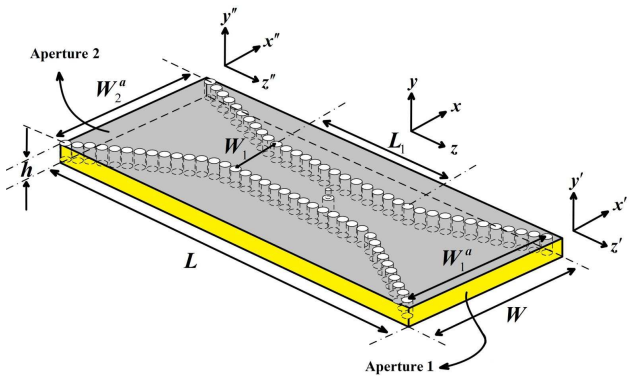

Figure 1. 3-D configuration of the proposed antenna.

of the horn are given as,

$$E_y(x') = E_0 \cos\left(\frac{(2n-1)\pi}{W^a_{1(eff)}}x'\right) e^{-jk\Delta(x')}$$
$$H_x(x') = -\frac{E_0}{\eta}\cos\left(\frac{(2n-1)\pi}{W^a_{1(eff)}}x'\right) e^{-jk\Delta(x')} \quad (1)$$

where η is the characteristic impedance of the substrate and $W^a_{1(eff)}$ the effective width of SIW structure at aperture of the proposed antenna which is obtained by empirical Equation (2) [15].

$$W_{eff} = W - 1.08\frac{d^2}{S} + 0.1\frac{d^2}{W}, \quad \eta = \sqrt{\frac{\mu_0}{\varepsilon_0\varepsilon_r}} \quad (2)$$

W, d, and S are center to center vias spacing, diameter of vias and the spacing between center to center adjacent vias, respectively [15]. The prime signs are used for indicating fields at the aperture of the horn. The necessity of the phase variation term is due to the cylindrical waves which are crossing through the flaring part. So the wave has travelled different distances from the apex (center of the coaxial excitation) to the aperture [27]. Hence, at any point on the aperture (x'), the phase of the field will not be the same as that at the origin. The difference in path of travel, is defined as $\Delta(x')$. It can be shown that the phase variations of dominant TE_{10} mode satisfies by the following quadratic expression,

$$\Delta(x') = \frac{x'^2}{2\rho'} \quad (3)$$

where ρ' is radial distance to the aperture of the horn ($L = 2\rho'$) which is equivalent to Equation (4).

$$\rho' = \rho_h \cos\psi_h \quad (4)$$

ψ_h and ρ_h are angular and length of the flaring part of the H plane horn antenna.

As the length of the flaring part increases, higher order modes are created. So phase variation should include higher order terms. However for simplicity, the impact of the higher order modes on phase variation can be neglected. To find the fields radiated by the horn, only the tangential components of the E- and H-fields over a closed surface at the aperture must be known. Considering closed surface coincide with an infinite plane passing through the mouth of the horn, surface equivalence theory can be applied to aperture of the proposed

antenna [27]. Approximate equivalent currents are determined as,

$$\begin{aligned} J_y(x') &= H_x(x') = -\frac{E_0}{\eta}\cos\left(\frac{(2n-1)\pi}{W^a_{1(eff)}}x'\right)e^{-jk\Delta(x')} \\ M_x(x') &= E_y(x') = E_0\cos\left(\frac{(2n-1)\pi}{W^a_{1(eff)}}x'\right)e^{-jk\Delta(x')} \end{aligned} \tag{5}$$

The fields and equivalent currents on the second aperture are determined similar to first one by knowing $W^a_{1(eff)} = W^a_{2(eff)}$. Finally, the radiated field can be obtained by using magnetic and electric potential vectors [27]. Therefore total electric and magnetic radiated fields can be written in terms of cosine and sine Fresnel integrals,

$$\begin{aligned} E^T_\theta = {} & j\frac{E_0 h}{4}\sqrt{\frac{k_0\rho'}{\pi\sqrt{\varepsilon_r}}}\sin\varphi\frac{\sin Y}{Y}\frac{e^{-jk_0r}}{r}\left[e^{j\frac{K'^2\rho'}{2k}}\ F(t'_1,t'_2)\right. \\ & \left.+e^{j\frac{K''^2\rho'}{2k}}F\left(t''_1,t''_2\right)\right]\left(\frac{1}{\sqrt{\varepsilon_r}}\cos\theta\cos\left(k_0\rho'\cos\theta\right)-j\sin\left(k_0\rho'\cos\theta\right)\right) \end{aligned} \tag{6}$$

$$\begin{aligned} E^T_\varphi = {} & j\frac{E_0 h}{4}\sqrt{\frac{k_0\rho'}{\pi\sqrt{\varepsilon_r}}}\cos\varphi\frac{\sin Y}{Y}\frac{e^{-jk_0r}}{r}\left[e^{j\frac{K'^2\rho'}{2k}}\ F(t'_1,t'_2)\right. \\ & \left.+e^{j\frac{K''^2\rho'}{2k}}F\left(t''_1,t''_2\right)\right]\left(\frac{1}{\sqrt{\varepsilon_r}}\cos\left(k_0\rho'\cos\theta\right)-j\cos\theta\sin\left(k_0\rho'\cos\theta\right)\right) \end{aligned} \tag{7}$$

$$\begin{aligned} H^T_\theta = {} & -j\frac{E_0 h}{4\eta_0}\sqrt{\frac{k_0\rho'}{\pi\sqrt{\varepsilon_r}}}\cos\varphi\frac{\sin Y}{Y}\frac{e^{-jk_0r}}{r}\left[e^{j\frac{K'^2\rho'}{2k}}\ F(t'_1,t'_2)\right. \\ & \left.+e^{j\frac{K''^2\rho'}{2k}}F\left(t''_1,t''_2\right)\right]\left(\frac{1}{\sqrt{\varepsilon_r}}\cos\left(k_0\rho'\cos\theta\right)-j\cos\theta\sin\left(k_0\rho'\cos\theta\right)\right) \end{aligned} \tag{8}$$

$$\begin{aligned} H^T_\varphi = {} & j\frac{E_0 h}{4\eta_0}\sqrt{\frac{k_0\rho'}{\pi\sqrt{\varepsilon_r}}}\sin\varphi\frac{\sin Y}{Y}\frac{e^{-jk_0r}}{r}\left[e^{j\frac{K'^2\rho'}{2k}}\ F(t'_1,t'_2)\right. \\ & \left.+e^{j\frac{K''^2\rho'}{2k}}F\left(t''_1,t''_2\right)\right]\left(\frac{1}{\sqrt{\varepsilon_r}}\cos\theta\cos\left(k_0\rho'\cos\theta\right)-j\sin\left(k_0\rho'\cos\theta\right)\right) \end{aligned} \tag{9}$$

where

$$\begin{aligned} F(t_1,t_2) &= [C(t_2)-C(t_1)]-j\,[S(t_2)-S(t_1)] \\ K' &= \frac{(2n-1)\pi}{W^a_{1(eff)}}+k_x, \quad K''=-\frac{(2n-1)\pi}{W^a_{1(eff)}}+k_x \\ k_x &= k_0\sin\theta\cos\varphi, \quad Y=\frac{k_0 h}{2}\sin\theta\sin\varphi \end{aligned} \tag{10}$$

$$t_1' = \frac{1}{\sqrt{\pi k\rho'}}\left(-k\frac{W^a_{1(eff)}}{2} - K'\rho'\right), \quad t_2' = \frac{1}{\sqrt{\pi k\rho'}}\left(+k\frac{W^a_{1(eff)}}{2} - K'\rho'\right)$$

$$t_1'' = \frac{1}{\sqrt{\pi k\rho'}}\left(-k\frac{W^a_{1(eff)}}{2} - K''\rho'\right), \quad t_2'' = \frac{1}{\sqrt{\pi k\rho'}}\left(+k\frac{W^a_{1(eff)}}{2} - K''\rho'\right)$$

3. EXCITATION OF THE PROPOSED ANTENNA

The proposed antenna has been excited through simple 50 ohm coaxial probe. In addition, impedance matching of different frequencies can be determined by the core length which pierced into the substrate. Moreover, flaring part and effective width of the waveguide part determine the operating frequencies. The fundamental cut off frequency of the waveguide part can be derived from Equation (11) [30].

$$f = c/\left(2W_{eff}\sqrt{\varepsilon_r}\right) \tag{11}$$

where effective width of the SIW structure is obtained from empirical Equation (2). In the waveguide, center to center vias spacing, diameter, and the distance between center to center adjacent vias are 10, 1, and 1.2 mm, respectively. So, first resonance of the antenna should occur after the fundamental cut off frequency 11.1 GHz.

As mentioned before, varying the separation between elements could create different patterns obtained by continuing the flaring part as a consequence of higher order modes excitation with their particular distribution in the structure. Different dimensions of the antenna are presented in Table 1, with respect to the distribution of electric field.

Table 1. Different dimensions of the proposed antenna (all dimensions are in mm).

Parameter	$W_1^a = W_2^a$	W_1	W	L_1	L
Case 1	18.57	10	19.57	16.8	32
Case 2	22.85	10	23.85	16.8	39.4
Case 3	28.57	10	29.57	16.8	49
Case 4	34.28	10	35.28	16.8	58.8
Case 5	41.42	10	42.42	16.8	70.8
Case 6	48.57	10	49.57	16.8	82.6

4. SIMULATION RESULTS

The satisfied resonances of the designed antenna depend on the feeding transition from coaxial to SIW structure. The simulated reflection

coefficients are shown in Figure 2 according to different core lengths and dimensions presented in Table 1. Additionally, 2-D gain patterns in both E-(yz) and H-(xz) planes are presented in Figure 3 according to different dimensions of the antenna and corresponding operating frequencies in Figure 2. Due to the symmetric configuration of the antenna, consequently symmetric radiation pattern, only half of the patterns are displayed in each E and H planes. As shown in the Figure 3, the peak gain of the antenna is higher than 5 dB and the nulls happen below -15 dB in each operating frequency. Furthermore, with respect to Figures 2 and 3, the nulls of the radiation pattern should change when the length or operating frequency of the antenna increases. In this case some nulls are added to radiation pattern due to the excitation of the TE_{n0} modes. Distribution of this modes in the

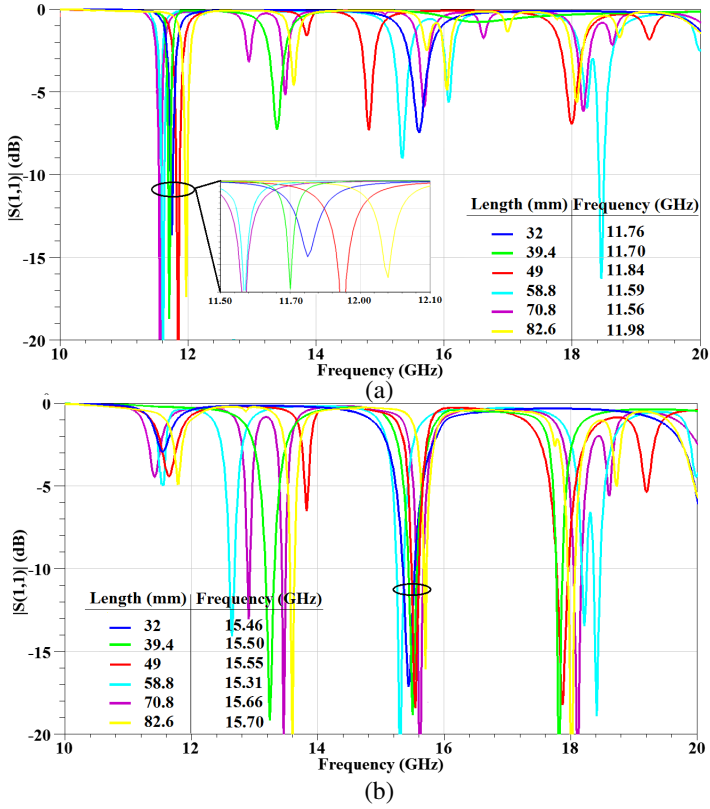

Figure 2. Simulated reflection coefficients of the antenna with: (a) coaxial core length 0.8 mm, (b) coaxial core length 1.2 mm.

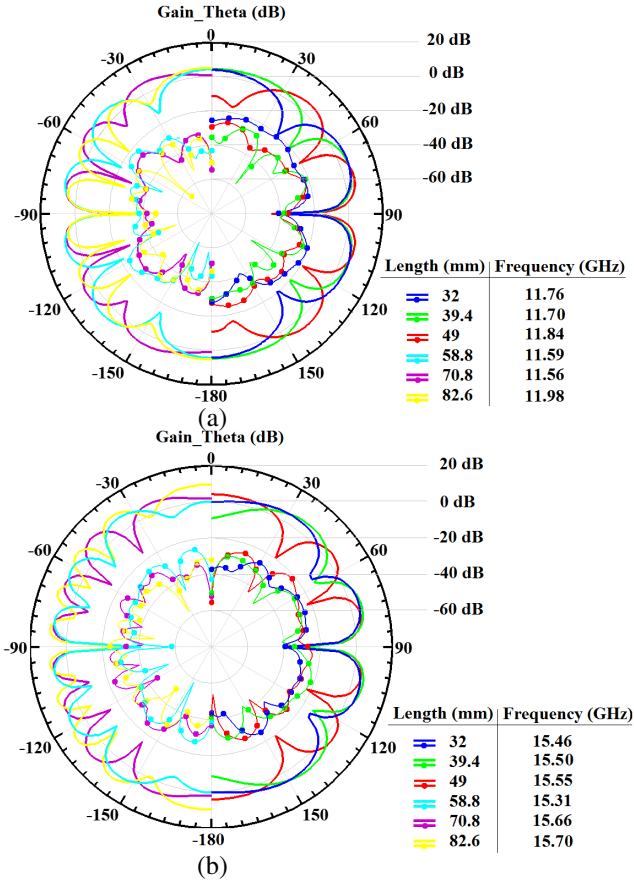

Figure 3. 2-D gain pattern of the antenna according to different lengths and corresponding operating frequencies with: (a) coaxial core length 0.8 mm, (b) coaxial core length 1.2 mm.

structure and corresponding 3-D total gain patterns are presented in Figure 4. According to Figure 4, if a higher order mode in contrast with one lower mode propagates in the structure, 4 nulls are added to the radiation pattern. but when the propagation of the higher order mode happens at the apertures of the antenna, 2 nulls are added to the radiation pattern. Furthermore, by attention to Equations (6) and (7), the proposed antenna has low cross-polarized radiation in both of the fundamental and higher order modes excitation, whereas most antennas exhibit high cross-polarized radiation at higher-order modes excitation.

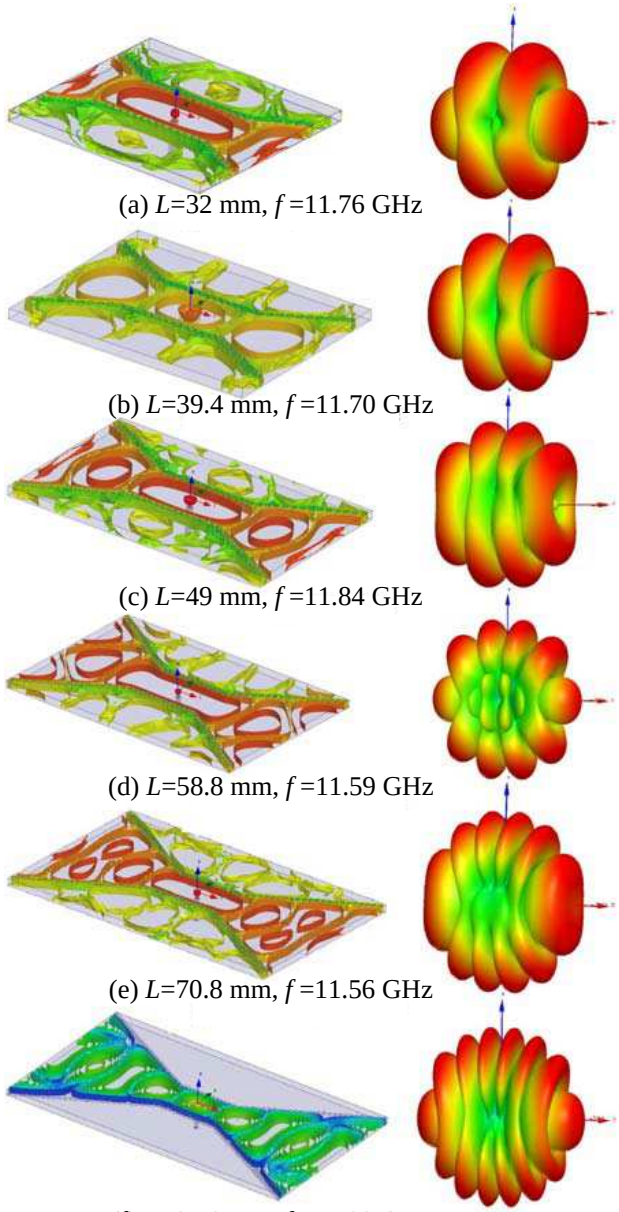

Figure 4. Distribution of electric fields in the structure and the corresponding 3-D total gain patterns.

5. COMPARISON BETWEEN THE THEORETICAL AND SIMULATION RESULTS

Far field components of the designed antenna in terms of electric and magnetic fields include both of E_θ, E_ϕ and H_θ, H_ϕ. In the principal E- and H-planes ($\varphi = \frac{\pi}{2}, 0$), the electric and magnetic fields only reduce to E_θ, H_ϕ and E_ϕ, H_θ, respectively. Considering Equation (6), comparison between simulation and theoretical results has been carried out based on normalized two-dimensional far-field E-plane amplitude patterns which are shown in Figure 5. Solid and symbolic lines are obtained from simulation and the proposed method, respectively. The little differences between simulation and theoretical results are due to two reasons: first, assuming role of SIW as a rectangular waveguide, second, approximation of the phase variation for higher order modes should include higher terms instead of quadratic estimation. However, theoretical result can determine the position of the nulls exactly as

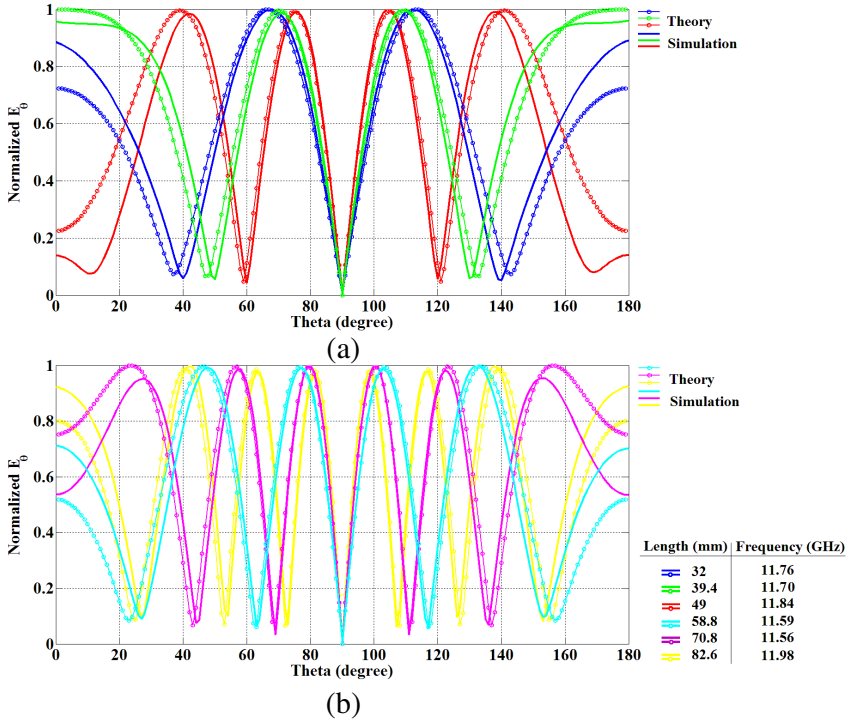

Figure 5. Comparison between simulation and theoretical results based on normalized E-plane radiation patterns according to different lengths: (a) 32, 39.4, and 49, (b) 58.8, 70.8, and 82.6 mm.

same as simulation results which is the most important part in this antenna design.

RF-MEMS switches are used to switch the radiation pattern from one vein to another one. In continuity, combination of the switches with proposed antenna have been investigated.

6. RF-MEMS SWITCHES

A critical component of the reconfigurable antenna is the switch used to connect or disconnect elements of the antenna. The insertion loss and isolation of the switches dictate the performance of the antenna. RF-MEMS switches have shown good RF characteristics such as inherent wide bandwidth, low insertion loss, and high isolation, which can be used at both low and high frequency applications [11]. 3-D geometry of the reconfigurable pattern antenna is presented in Figure 6. Structure

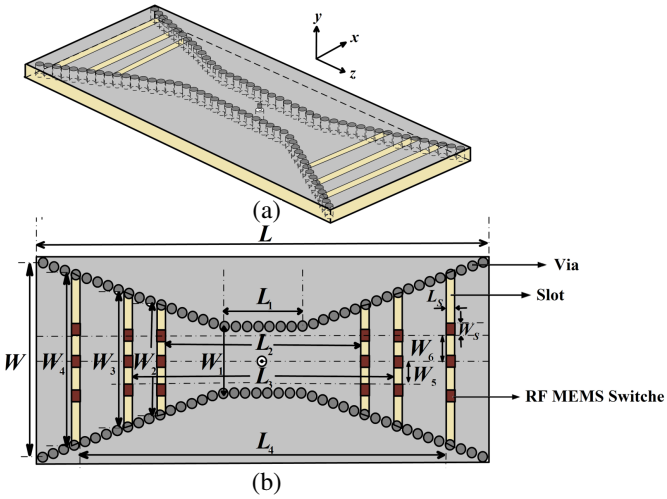

Figure 6. (a) 3-D configuration of the proposed reconfigurable pattern antenna, (b) top view of this antenna with RF-MEMS switches.

Table 2. Dimensions of the proposed reconfigurable antenna.

Parameter	W	W_1	W_2	W_3	W_4	W_5	W_6
Value (mm)	34.28	10	18.57	22.85	28.57	4	6
Parameter	W_s	L	L_1	L_2	L_3	L_4	L_s
Value (mm)	3	58.8	16.8	32	39.4	49	2.5

of the antenna consists of horizontal slots and switches between them on top and bottom of the substrate. The width of the slots are 2.5 mm. Other dimensions are presented in Table 2. The switches can be turned on/off in order to reconfigure the radiation properties by changing the effective electrical length. More specifically, position of the switches should be chosen carefully to couple weakly/strongly to other elements in OFF/ON state. The configuration of switches is shown in Figure 6(b). Three switches are installed along the gap, one in the middle and two others between the vias and the middle one. The positions of the offset switches should be chosen based on current distribution corresponding to distribution of TE_{n0} modes in the structure in order to conduct maximum current to the next slot. The spacing between the slots are chosen similar to Section 4 in order to cover the previous results. It is evident that for the similar operating

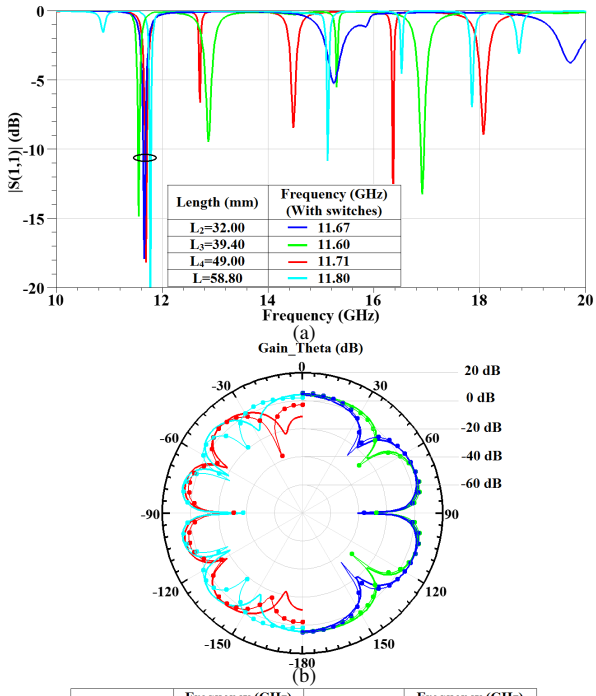

Figure 7. Simulated: (a) reflection coefficients, (b) 2-D gain patterns of the reconfigurable antenna according to operating frequencies.

frequencies, the spacing between the last apertures determines the maximum multiplicity of the nulls in the far field radiation pattern. The simulated results of the reconfigurable antenna are presented in Figure 7. Only four cases have been considered in reconfigurable antenna due to more switches requirement by increasing the length of the slots. Considering Figure 7, negligible frequency and pattern deviation is introduced by using RF-MEMS switches. This deviation is due to open spaces between the slots. The results show that whole of the antenna can be fabricated on a single substrate to reconfigure pattern. It is obvious that if no needs to reconfigure pattern, satisfied radiation pattern can be obtained without using any switches.

7. EXPERIMENTAL RESULTS

Considering the characteristics of SIW structure, replacing the substrate of the proposed antenna with another one, only changes the operating frequencies as a result of altering in fundamental cut off frequency. Therefore, the pattern reconfigurable characteristic of the proposed antenna is not dependent on specific substrate. Hence, due to the availability of test equipments and inexpensive FR4 substrate, prototype was fabricated on FR4 substrate to validate the proposed antenna. Obviously, if operating frequencies are altered, the number of the nulls in the far field radiation pattern vary as presented in Figure 3. The entire structure over FR4 substrate was simulated, fabricated, and measured. Available Radant MEMS SPST-RMSW100 packaged switches were used for achieving reconfigurability. The overall outer dimension of this switch is 1.5 mm × 1.5 mm × 0.25 mm with a gold base. Copper pads with dimensions similar to the size of the switch (1.5 mm × 1.5 mm) were etched on the slot. The RF-MEMS switches glued onto the copper pads and wire are bonded to the substrate (1 mil diameter aluminum wire). The source and drain terminals of

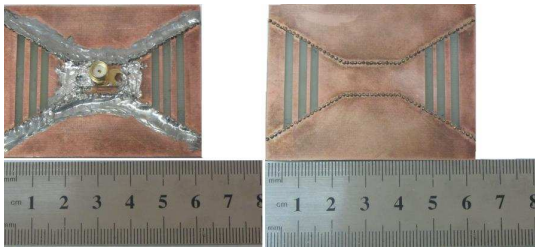

Figure 8. Figures of the fabricated antenna without implementation of switches on it.

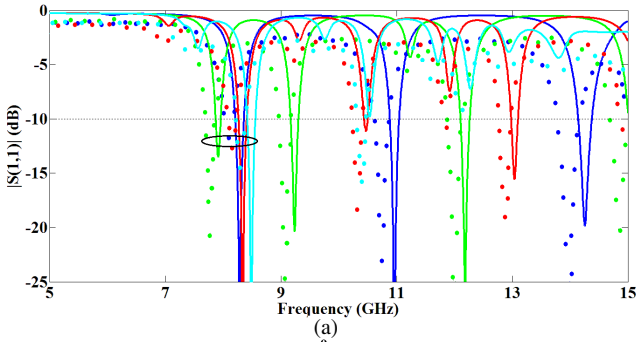

Length (mm)	Frequency (GHz) (Simulation)	Length (mm)	Frequency (GHz) (Measurement)
L_2=32.00	8.29	L_2=32.00	8.10
L_3=39.40	7.92	L_3=39.40	7.78
L_4=49.00	8.34	L_4=49.00	8.16
L=63.60	8.49	L=63.60	8.32

Figure 9. Simulated and measured: (a) reflection coefficients and (b) radiation patterns for the proposed reconfigurable pattern antenna.

the switch are wire bonded across the slot with two wire bonds each, and the gate terminal is wire bonded to the DC isolation layer [31]. After calibrating the network analyser, reflection coefficients of the proposed antenna were measured when different combinations of the switches were activated. Figure 8 shows the fabricated proposed antenna without implementation of switches on it. It should be noted that the device was made only for the research purposes and since we had access to limited number of RF-MEMS switches than actually were needed for the antenna, in each measurement, the same switches had to be used. In other words, for each measurement the available switches were placed across the slot, and to perform the next measurement, those switches were taken out and placed on different appropriate position. This multiple usage of the available switches would require several soldering so that the final fabricated

prototype was not suitable for insertion in the paper. As a result, here the fabricated prototype, without the placement of the RF-MEMS switches, is presented. The simulated and measured reflection coefficients and radiation patterns are shown in Figure 9. In the results of the measurements, the frequencies shift between the simulated and measured reflection coefficients are attributed to the fabrication accuracy, particularly to the substrate used in fabrication and precision of jointing used to join the feed and the antenna. However, measured and simulated results are in good agreement with each other which validate the simulation results.

8. CONCLUSION

A novel pattern reconfigurable antenna based on SIW technology and RF-MEMS switches has been proposed. Simulation results of the proposed antenna are compared with the theoretical and measured results which demonstrate the validation of the proposed antenna. The antenna can be fabricated on single substrate with satisfied pattern and frequency or with RF-MEMS switches for reconfigurable applications. The merits of the proposed antenna are: compatibility with PCB structure, single excitation, low profile, low cross polarization, high gain, compact form, capability of operating at different frequencies and reconfigurable radiation pattern by using RF-MEMS switches.

REFERENCES

1. Choi, J. and S. Lim, "Frequency and radiation pattern reconfigurable small metamaterial antenna using its extraordinary zeroth-order resonance," *Journal of Electromagnetic Waves and Applications*, Vol. 24, Nos. 14–15, 2119–2127, 2010.
2. Chen, B., T. Chen, Y. Jiao, and F. Zhang, "A reconfigurable microstrip antenna with switchable polarization," *Journal of Electromagnetic Waves and Applications*, Vol. 20, No. 10, 63–68, 2006.
3. Lin, S.-Y., Y.-C. Lin, and J.-Y. Lee, "T-strip fed patch antenna with reconfigurable polarization," *Progress In Electromagnetics Research Letters*, Vol. 15, 163–173, 2010.
4. Zhang, S., G. H. Huff, J. Feng, and J. T. Bernhard, "A pattern reconfigurable microstrip parasitic array," *IEEE Trans. Antennas Propagat.*, Vol. 52, 2773–2776, 2004.
5. Ali, M. T., M. N. M. Tan, A. R. B. Tharek, M. R. B. Kamarudin, M. F. Jamlos, and R. Sauleau, "A novel of reconfigurable planar

antenna array (RPAA) with beam steering control," *Progress In Electromagnetics Research B*, Vol. 20, 125–146, 2010.

6. Monti, G., L. Corchia, and L. Tarricone, "Planar bowtie antenna with a reconfigurable radiation pattern," *Progress In Electromagnetics Research C*, Vol. 28, 61–70, 2012.
7. Kamarudin, B., P. Hall, F. Colombel, and M. Himdi, "Electronically switched beam disk-loaded monopole array antenna," *Progress In Electromagnetics Research*, Vol. 101, 339–347, 2010.
8. Cheng, Y. J., "Substrate integrated waveguide frequency-agile slot antenna and its multibeam application," *Progress In Electromagnetics Research*, Vol. 130, 153–168, 2012.
9. Kang, W., K. H. Ko, and K. Kim, "A compact beam reconfigurable antenna for symmetric beam switching," *Progress In Electromagnetics Research*, Vol. 129, 1–16, 2012.
10. Pourziad, A., S. Nikmehr, and H. Veladi, "A novel multi-state integrated RF MEMS switch for reconfigurable antennas applications," *Progress In Electromagnetics Research*, Vol. 139, 389–406, 2013.
11. Rebeiz, G. M., *RF MEMS: Theory, Design and Technology*, Wiley, New York, 2003.
12. Brown, E., "RF-MEMS switches for reconfigurable integrated circuit," *IEEE Trans. Microw. Theory Tech.*, Vol. 46, 1998.
13. Brown, E. R., "On the gain of a reconfigurable-aperture antenna," *IEEE Trans. Antennas Propagat.*, Vol. 49, 1357–1362, 2001.
14. Raedi, Y., S. Nikmehr, and A. Pourziad, "A novel bandwidth enhancement technique for X-band RF MEMS actuated reconfigurable reflectarray," *Progress In Electromagnetics Research*, Vol. 111, 179–196, 2011.
15. Xu, F. and K. Wu, "Guided waves and leakage characteristics of substrate integrated waveguides," *IEEE Trans. Microw. Theory Tech.*, Vol. 53, No. 1, 66–73, 2005.
16. Deslandes, D. and K. Wu, "Accurate modeling, wave mechanisms, and design considerations of substrate integrated waveguide," *IEEE Trans. Microw. Theory Tech.*, Vol. 54, 2516–2526, 2006.
17. Salehi, M. and E. Mehrshahi, "A closed-form formula for dispersion characteristics of fundamental SIW mode," *IEEE Microw. Wireless Compon. Lett.*, Vol. 21, 4–6, 2011.
18. Zhang, Z. G., Y. Fan, Y. J. Cheng, and Y.-H. Zhang, "A novel multilayer dual-mode substrate integrated waveguide complementary filter with circular and elliptic cavities," *Progress*

In Electromagnetics Research, Vol. 127, 173–188, 2012.

19. Wu, D., Y. Fan, M. Zhao, and B. Zheng, "Vertical transition and power divider using via walled circular cavity for multilayer millimeter wave module," *Journal of Electromagnetics Waves and Applications*, Vol. 23, Nos. 5–6, 729–735, 2009.
20. Che, W., E. Yung, K. Wu, and X. Nie, "Design investigation on millimeter-wave ferrite phase shifter in SIW," *Progress In Electromagnetics Research*, Vol. 45, 263–275, 2004.
21. Bakhtafrooz, A., A. Borji, D. Busuioc, and S. Safavi-Naeini, "Novel two-layer millimeter-wave slot array antennas based on substrate integrated waveguides," *Progress In Electromagnetics Research*, Vol. 109, 475–491, 2010.
22. Lee, S., S. Yang, A. E. Fathy, and A. Elsherbini, "Development of a novel UWB vivaldi antenna array using SIW technology," *Progress In Electromagnetics Research*, Vol. 90, 369–384, 2009.
23. Djera, T. and K. Wu, "Corrugated substrate integrated waveguide (SIW) antipodal linearly tapered slot antenna array fed by quasi-triangular power divider," *Progress In Electromagnetics Research C*, Vol. 26, 139–151, 2012.
24. Cheng, Y. J., W. Hong, and K. Wu, "Design of a Monopulse antenna using a dual V-type linearly tapered slot antenna (DVLTSA)," *IEEE Trans. Antennas Propagat.*, Vol. 56, 2903–2909, 2008.
25. Cheng, S., H. Yousef, and H. Kratz, "79 GHz slot antennas based on substrate integrated waveguides in a flexible printed circuit board," *IEEE Trans. Antennas Propagat.*, Vol. 57, 64–70, 2009.
26. Kazemi, R., A. E. Fathy, and R. A. Sadeghzadeh, "Dielectric rod antenna array with substrate integrated waveguide planar feed network for wideband applications," *IEEE Trans. Antennas Propagat.*, Vol. 60, No. 3, 1312–1319, 2012.
27. Balanis, C. A., *Antenna Theory Analysis and Design*, Wiley, 2005.
28. Wang, H., D.-G. Fang, B. Zhang, and W.-Q. Che, "Dielectric loaded substrate integrated waveguide H-plane horn antennas," *IEEE Trans. Antennas Propagat.*, Vol. 58, 640–647, 2010.
29. Mallahzadeh, R. and S. Esfandiarpour, "Wideband H-plane horn antenna based on ridge substrate integrated waveguide (RSIW)," *IEEE Antennas Wireless Propagat. Lett.*, Vol. 11, 85–88, 2012.
30. Pozar, D., *Microwave Engineering*, 3rd Edition, Wiley, 2005.
31. Rajagopalan, H., Y. Rahmat-Samii, and W. A. Imbriale, "RF MEMS actuated reconfigurable reflectarray patch-slot element," *IEEE Trans. Antennas Propagat.*, Vol. 56, 3689–3699, 2008.